Two-photon characterisation of long-Stokes-shift dye ATTO 490LS for single-laser multicolour imaging

King Yee Cheung ORCID [1], Yue Wu ORCID [2], Shu Ying Lee ORCID [2], Xianyuan Zhang ORCID [1], Masahiro Fukuda ORCID [1], Danesha Devini Suresh ORCID [1], Adam Claridge-Chang ORCID [1,3,4,5]

1. Programme in Neuroscience and Behavioural Disorders, Duke-NUS Medical School, Singapore
2. Microscopy Core Facility — Multiphoton Microscopy Unit, Yong Loo Lin School of Medicine, National University of Singapore, Singapore
3. Institute of Molecular and Cell Biology, A*STAR, Singapore
4. Department of Physiology, Yong Loo Lin School of Medicine, National University of Singapore, Singapore
5. Corresponding author: claridge-chang.adam@duke-nus.edu.sg

Abstract

Long-Stokes-shift fluorophores enable high sensitivity and multiplexed imaging with single-wavelength excitation. Under single-photon illumination ATTO 490LS exhibits a 165-nm Stokes shift, but its two-photon properties remain uncharacterised. Emission and excitation spectral analyses of ATTO 490LS in ex vivo *Drosophila melanogaster* brains identified two-photon excitation sensitivity at 940 nm, with peak emission at 640 nm. We demonstrate successful duplexed imaging of ATTO 490LS alongside Alexa Fluor 488 using a single 920-nm fibre laser and dual photomultiplier tubes, enabling distinct measurement of red and green fluorescence signals. These findings establish ATTO 490LS as suitable for multicolour two-photon microscopy with single-laser systems.

Figure

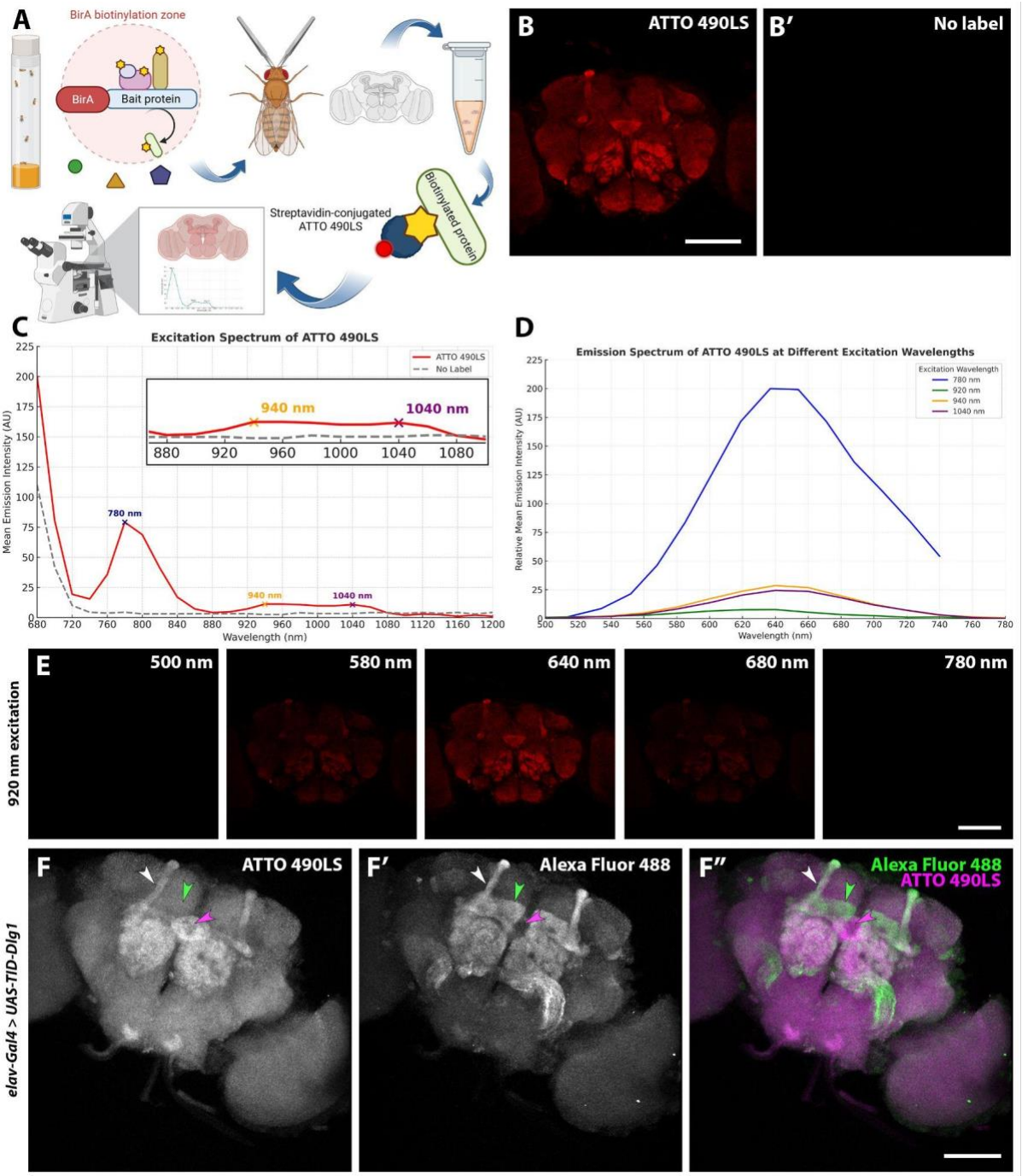

Figure 1. ATTO 490LS is excited by a 920 nm laser and is suitable for single-laser multicolour two-photon imaging.

(A) Schematic diagram of the experimental workflow. **(B)** Representative image of *elav-Gal4>UAS-TID-Dlg1* fly brain, with ATTO 490LS staining at 780 nm excitation during the excitation scan. Scale bar = 100 µm. **(B′)** The identical experiment as **B**, but with no staining. **(C)** Normalised excitation spectrum of ATTO 490LS (red line) over 680 nm to 1200 nm compared with the emission intensity from an unlabelled brain (grey dashed line). Emission intensity from 680–740nm excitation is almost entirely attributed to autofluorescence. Emission intensity of ATTO 490LS peaks at 780 nm, 940 nm, and 1040 nm excitation, with normalised mean fluorescence intensities of 79.1, 11.1, and 10.71

(arbitrary units) respectively. Insert shows an enlarged view of the emission peaks at 940 nm and 1040 nm, which are 3–4-fold higher than the baseline emission intensity. **(D)** Normalised emission spectra of ATTO 490LS over 500 nm to 780 nm, at 780 nm (blue line), 920 nm (green line), 940 nm (orange line), and 1040 nm (burgundy line) excitation. Excitation at all four tested wavelengths gives emission peaks at 640 nm, with normalised mean fluorescence intensities of 200.0, 7.5, 28.1, and 24.1 (arbitrary units) respectively. **(E)** Respective images at various emission wavelengths of an ATTO 490LS-stained *elav-Gal4>UAS-TID-Dlg1* brain from the 920 nm excitation emission scan. Scale bar = 100 µm. **(F–F′′)** Maximum intensity projection images of an ATTO 490LS- and Alexa Fluor 488-coupled-anti-c-Myc tag antibody-stained *elav-Gal4>UAS-TID-Dlg1* brain. Both fluorophores were simultaneously excited by the 920 nm laser at 3% power (30 mW). Detection of **(F)** ATTO 490LS signals with the red-filtered PMT at 1% gain, **(F′)** detection of Alexa Fluor 488 signals with the green-filtered PMT at 5% gain, and **(F′′)** merged signals. Magenta arrowheads mark the ellipsoid body, an example structure labelled here only by ATTO 490LS. Green arrowheads mark the γ-lobe of the mushroom body, an example structure labelled here only by Alexa Fluor 488. White arrowheads mark the α-lobe of the mushroom body, an example structure double-labelled here by both ATTO 490LS and Alexa 490LS. Scale bar = 100 µm.

Description

A Stokes shift refers to the difference in wavelength between maximum absorption and maximum emission of a fluorophore (Stokes, 1852). A long Stokes shift describes when a fluorescent molecule is excitable by a relatively short wavelength, but emits at a much longer wavelength due to a loss of energy following excitation (Lakowicz, 2001; Valeur, 2001). This can be valuable in fluorescence microscopy, as it reduces overlap between excitation and emission spectra, thereby minimising noise from scattered excitation light and improving detection sensitivity (Sednev et al., 2015; Liu et al., 2024).

Long-Stokes-shift fluorophores can also be suitable for multicolour imaging on microscope systems that are limited to a single laser. A long-Stokes-shift dye can be combined with another fluorophore with the same or a similar excitation profile, but give a completely different emission spectrum, thus making the two dyes distinguishable during image collection (Likhotkin et al., 2023). ATTO 490LS (ATTO-TEC GmbH) is an example of a red-fluorescing long-Stokes-shift dye, with a reported single-photon excitation wavelength of 496 nm and emission wavelength of 661 nm (Stokes shift of 165 nm). It has been used in conjunction with other common dyes such as ATTO 488, ATTO 514, Alexa Fluor 488, 594, and 647 (Reitz et al., 2021).

We are interested in utilising a long-Stokes-shift fluorophore for in vivo *Drosophila* brain two-photon imaging alongside genetically encoded indicators, for example GCaMP, which fluoresce green with an emission peak wavelength of 510 nm (Nakai et al., 2001; Zhang et al., 2023) when excited by, for example, a 920 nm ultrashort pulse laser. Under single-photon conditions, ATTO 490LS has a similar excitation peak to GFP and its derived sensors like the GCaMPs, making ATTO 490LS a potential reference dye during neuronal imaging. However, ATTO 490LS's two-photon properties have not yet been tested nor reported in literature. Here, we perform emission and excitation spectral analyses of streptavidin-conjugated ATTO 490LS to determine the dye's suitability for two-photon imaging with systems that are configured with only a single fixed-wavelength 920 nm fibre laser, but have at least two detectors (Figure 1A).

To determine the optimal two-photon wavelength for exciting ATTO 490LS, we first performed an excitation scan on stained fly brains, which involved measuring emission intensity while adjusting the excitation wavelength. The resulting emission intensity peaked at 780 nm, 940 nm, and 1040 nm excitation, with normalised relative mean fluorescence intensities of 79.1, 11.1, and 10.7 arbitrary units, respectively (Figure 1B, C). Emission was also detected in the 680–740 nm excitation range, however this could be almost entirely attributed to autofluorescence (Figure 1B′, C). The largest of these three emission peaks occurred at 780 nm excitation, thus indicating that is the most efficient laser wavelength within the tested range for maximum emission of the dye. As it is not necessary to excite at the global excitation maxima, and given that we are interested in assessing the dye for compatibility with GFP excitation, the second local maxima at 940 nm was promising as this is within close range of the commercially available fibre laser wavelength of 920 nm.

Additionally, longer excitation wavelengths generate less autofluorescence signals, thus excitation at 920 nm is a more attractive option than at 780 nm.

To confirm that the wavelengths identified in the excitation scan are sufficient to excite ATTO 490LS and to verify the emission spectrum under two-photon illumination, we performed a series of emission scans. We measured the intensities of emission at different wavelengths while keeping the excitation wavelength fixed at one of the three local maxima. An emission scan was also done for 920 nm excitation. At all four tested excitation wavelengths, emission intensities peaked at 640 nm (Figure 1D, E), which is similar to the manufacturer's reported emission wavelength of 661 nm under single-photon excitation. The normalised relative mean fluorescence intensities concurred with the excitation-scan readings, where 780 nm excitation led to the highest emission intensity (200.0 arbitrary units), while 920 nm excitation resulted in a lower emission intensity (7.5 arbitrary units). Taken together, results from both excitation and emission scans suggest that ATTO 490LS can be excited using a 920 nm two-photon laser and will emit at around 640 nm.

To assess the actual utility of ATTO 490LS with the type of microscope widely used for *Drosophila* two-photon imaging, we prepared ex vivo *elav-Gal4>UAS-TID-Dlg1* brains double-labelled with streptavidin-conjugated ATTO 490LS and anti-c-Myc tag primary antibody coupled with an Alexa Fluor 488 secondary. Discs large 1 (Dlg1) is a crucial scaffolding protein, encoded by the *dlg1* gene in *Drosophila* (orthologous to the *DLG1*/*SAP97* gene in humans), and is a synaptic marker (Lahey et al., 1994; Woods et al., 1996). Here, *elav-Gal4* drives expression of the *UAS-TurboID-Dlg1* responder expressing the bait protein, which is tagged with the artificial peptide sequence Myc-tag, in post-mitotic neurons. Antibody staining against c-Myc will label TurboID-Dlg1, and is therefore expected to label generic neuronal scaffolding such as the post-synaptic density in the *Drosophila* brain. Meanwhile, staining with a streptavidin-conjugated dye will label any biotinylated proteins that are within a ~15 nm proximity to TurboID-Dlg1 (Branon et al., 2018). The brains were imaged with an early model Thorlabs A-SCOPE two-photon microscope equipped with a fixed-wavelength 920 nm fibre laser. We observed strong ATTO 490LS signals through the red-filtered photomultiplier tube (PMT; bandpass filter at 570–640 nm) and were able to identify labelled structures such as the antennal lobes, ellipsoid body, and the α- and β-lobes of the mushroom bodies (Figure 1F).

To examine the simultaneous detection and distinguishability of red and green signals excited by a single 920 nm laser, we turned our focus to the signal collected by the green-filtered PMT (bandpass filter at 500–550 nm). Distinct signals from each fluorophore could be observed (Figure 1F–F″, see also Extended Data); for example, the ellipsoid body is exclusively labelled by ATTO 490LS (see magenta arrowhead), the γ-lobes of the mushroom bodies are exclusively labelled by Alexa Fluor 488 (see green arrowheads), while the α- and β-lobes of the mushroom bodies and antennal lobes are double-labelled by both dyes (see white arrowheads). We establish that ATTO 490LS can be combined with Alexa Fluor 488 for duplexed imaging with a single 920 nm laser. Duplexed imaging with other fluorophores such as GCaMP should therefore also be possible.

In conclusion, we have characterised the two-photon optical properties of ATTO 490LS and demonstrated its utility for multicolour imaging with single-laser systems. The dye's compatibility with standard 920 nm excitation substantially lowers technical barriers to duplexed two-photon microscopy, particularly for laboratories with legacy equipment. We aim to eventually engineer ATTO 490LS-conjugated ligands for HaloTag, SNAP-tag, and other tag proteins (Los et al., 2008; Marques et al., 2022) for in vivo chemogenetic labelling in transgenic *Drosophila* lines, enabling simultaneous imaging of GCaMP calcium transients (or other green sensors (Liu et al., 2022; Hao et al., 2024)) alongside a stable red dye for use as a structural marker or sensor denominator. Such a tool may have relative benefits compared to (or simply provide another option to) inherently fluorescent proteins with long Stokes shifts (Kim et al., 2022; Subach et al., 2022). By expanding the toolkit for multicolour two-photon imaging in *Drosophila* and other systems, this work creates new opportunities for integrating functional imaging with genetic and behavioural analyses, advancing our capacity to dissect neural circuit function in behaving animals.

Methods

Drosophila lines and rearing

A cross of female virgin ☿ pan-neuronal driver *elav-Gal4 (X)* (Bloomington *Drosophila* Stock Centre, Stock #458) and male ♂ TurboID direct fusion bait *UAS-TID-Dlg1 Drosophila melanogaster* flies were set up on standard food supplemented with dry yeast and flipped every 2–3 days onto fresh food with yeast. Offspring were transferred to food containing 50 µM biotin for 5 days, which led to biotinylation of proteins proximal to the TurboID-Dlg1 bait proteins (following the principles of BioID proximity labelling (Branon et al., 2018)), and allowed for subsequent binding of the streptavidin-conjugated dye to the biotinylated proteins (Figure 1A).

Brain dissection and sample preparation

Biotin-fed *elav-Gal4>UAS-TID-Dlg1* flies were immobilised on ice and culled in ice-cold 70% ethanol for a few seconds. Flies were transferred to a SYLGARD 184-coated (Dow Corning) Petri dish, and brains were dissected in ice-cold 1× PBS using Dumont #5SF forceps (Fine Science Tools).

Dissected brains were fixed in 4% PFA in PBS-0.3% Triton X-100 for 20 minutes at room temperature and subsequently washed in PBS-0.3% Triton X-100 three times for 15 minutes at room temperature.

ATTO 490LS staining

1 mg of desiccated streptavidin-conjugated ATTO 490LS (ATTO-TEC GmbH, product no. AD 490LS) was resuspended in 1 ml of MilliQ water to form a stock solution of 1 mg/ml. Stock solution was aliquoted and stored protected from light at -40°C.

Based on standard *Drosophila* brain immunohistochemistry protocols and a protocol for ATTO staining of 50 µm-thick fixed mouse brain slices (Reitz et al., 2021), samples were incubated in ATTO 490LS at a concentration of 1:200 in PBS-0.3% Triton X-100 for 48 hours in the dark at 4°C. The streptavidin-conjugated dye will bind to and label biotinylated proteins that are proximal to the TurboID-Dlg1 bait protein (Figure 1A). The dye was removed, and the samples were washed in PBS-0.3% Triton X-100 four times for 15 minutes at room temperature. Samples can be stored in PBS at 4°C for a few weeks before proceeding with mounting and imaging.

Immunohistochemistry

For single-label antibody staining, an anti-c-Myc tag mouse monoclonal IgG_1 primary antibody (Santa Cruz Biotechnology, catalogue no. sc-40) was added to the samples at a concentration of 1:200 in PBS-0.3% Triton X-100 for 48 hours at 4°C. For double-label staining, the primary antibody was added alongside ATTO 490LS. Samples were washed in PBS-0.3% Triton X-100 three times for 15 minutes at room temperature. Alexa Fluor 488 goat anti-mouse IgG secondary antibody (Invitrogen ThermoFisher, catalogue no. A11001) was added at a concentration of 1:500 and samples were incubated overnight in the dark at 4°C. Samples were washed in PBS-0.3% Triton X-100 four times for 15 minutes at room

temperature. Samples can be stored in PBS at 4°C for a few weeks before proceeding with mounting and imaging.

Emission and excitation spectral scanning

Samples were mounted on 1.0–1.2 mm-thick 25 × 75 mm glass slides (Biomedia) in PBS and sealed with 170 µm-thick 18 × 18 mm glass cover slips. Mounting media were excluded to prevent potential effects they may have on the excitation and emission scan readings. Excitation and emission scans were performed on a Leica TCS SP8 DIVE multiphoton microscope (Leica Microsystems, Wetzlar, Germany) equipped with a tuneable femtosecond pulsed multiphoton laser. Samples were imaged using an HC FLUOTAR L 25×/0.95 W Corr water immersion objective. Emission light was collected using Leica HyD photodetector.

For excitation scans (Λ, capital lambda), the laser wavelength was sequentially stepped from 680 nm to 1200 nm in 20 nm defined increments, while keeping the emission bandwidth between 500 nm and 685 nm. Power output delivered to the microscope remained constant at 65 mW ± 5 mW using the 'Constant Power' excitation control mode. For emission scans (λ, lowercase lambda), the excitation wavelengths were fixed at 780 nm, 920 nm, 940 nm, or 1040 nm. The emission detection bandwidth was sequentially stepped from 500 nm to 780 nm with a step size of 20 nm, with the exception of the scan at 780 nm excitation where the detection bandwidth was set to 500 nm to 740 nm (with a stepsize of 17–18 nm) due to limitations in collecting emission wavelengths that are too close to the excitation wavelength. Laser power setting (1%), detector gain (50), scan speed (200 Hz), and zoom (1×) were kept constant across all emission scans. Image acquisition and spectral detection were controlled using Leica LAS X software.

To quantify and compare emission intensities, each pixel of the subsequent 8-bit images was assigned a fluorescence intensity value from 0 to 255, where 0 represented no signal and 255 represented clipped or oversaturated signal (Shiffman, 2015), and a mean average of all pixels in the image were taken. Excitation and emission spectra graphs were generated using OpenAI by plotting normalised mean fluorescence intensity against excitation or emission wavelength, respectively.

Two-photon imaging

Samples were mounted on 1.0–1.2 mm-thick 25 × 75 mm glass slides (Biomedia) in VECTASHIELD Antifade Mounting Medium (Vector Laboratories Inc.) and sealed with 170 µm-thick 18 × 18 mm glass cover slips. *Z*-stack image series were taken on two different Thorlabs microscopes (Thorlabs, NJ, USA).

The first setup was a factory-built Thorlabs multi-photon microscope (2010 model, referred to here as "A-SCOPE") integrated with a Nikon Eclipse FN1 upright stand, a 7.9 kHz resonant/galvo scan head, a 1W FemtoFiber Ultra 920 laser (Toptica, Munich, Germany), a XLUMPLFLN 20× water immersion objective lens (Olympus, Tokyo, Japan), GaAsP PMT detectors, and ThorImageLS software (Thorlabs, NJ, USA). Laser power was set to 30 mW, unless stated otherwise. Emission light was collected by the green-filtered PMT,

223 with a bandpass filter of 525/50 nm, and the red-filtered PMT, with a bandpass filter of
224 605/70 nm. Detector gains were set to 5% and 1% for the green- and red-filtered PMTs
225 respectively, unless stated otherwise.

226 The second imaging setup was a Thorlabs B-SCOPE, equipped with CFI75 Apochromat
227 25×C W water immersion objective lens (Nikon, Tokyo, Japan) and Mai Tai eHP DS (Spectra
228 Physics, CA, USA) running at 920 nm at 22.1 mW power. We used a set of 562LP and 635LP
229 dichroic mirrors (Chroma) and 525/50 nm and 607/70 nm filters (Chroma) for the green
230 and red channels respectively. Detector gains were set to 5% for the green and 1% for the
231 red channel.

232 **Image processing**

233 The two-photon image stacks were subjected to Gaussian blur 3D processing (X: 0, Y:0,
234 Z:2) and maximum intensity projection processing in Fiji (Schindelin et al., 2012). For the
235 purpose of visualising dual-channel images, signal collected by the green-filtered PMT was
236 pseudo-coloured to green, while signal collected by the red-filtered PMT was pseudo-
237 coloured to magenta. 3D rendered movies were created using the 3D Viewer plugin
238 (Schmid et al., 2010) on Fiji.

239 The schematic diagram was created in BioRender. The figure was assembled in Adobe
240 Photoshop.

241 **Reagents**

Animal Species	**Genotype**	**Available From**
Drosophila melanogaster	*elav-Gal4 (X)*	Bloomington *Drosophila* Stock Centre (Stock #458)
Drosophila melanogaster	*UAS-TID-Dlg1*	Gift from Gunnar Poplawski and Keshika Ravichandran, manuscript in preparation.

242

Reagent/Antibody	**Description**	**Available From**
ATTO 490LS	Streptavidin-conjugated	ATTO-TEC GmbH (product no. AD 490LS)
anti-c-Myc tag (9E10)	Mouse monoclonal IgG_1	Santa Cruz Biotechnology (catalogue no. sc-40)
Alexa Fluor 488	Goat anti-mouse IgG (H+L)	Invitrogen ThermoFisher (catalogue no. A11001)

243

Extended Data

Extended Data Figure 1. Duplexed two-photon imaging of *Drosophila* brain stained with ATTO 490LS and Alexa Fluor 488.

Resource Type: Image

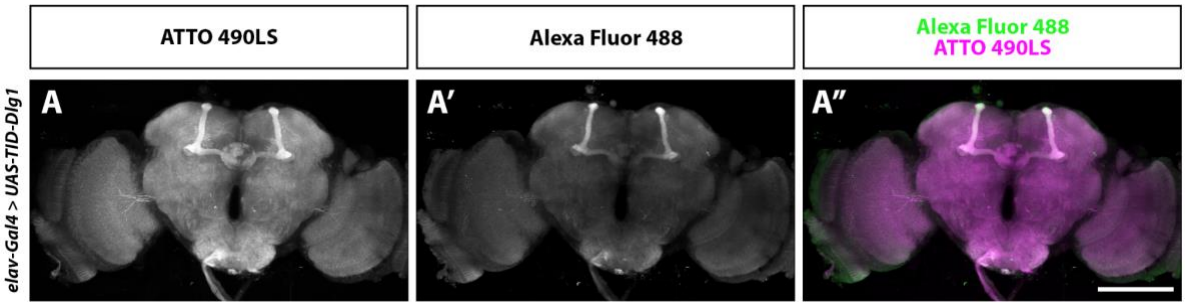

(A–A″) Maximum intensity projection images of an ATTO 490LS- and Alexa Fluor 488-coupled-anti-c-Myc tag antibody-stained *elav-Gal4>UAS-TID-Dlg1 Drosophila* brain. Both fluorophores were simultaneously excited by the 920 nm laser at 22.1 mW power under the objective lens. *Z*-stack series was imaged from the posterior to the anterior side. Detection of **(A)** ATTO 490LS signals with the red-filtered PMT at 1% gain, **(A′)** detection of Alexa Fluor 488 signals with the green-filtered PMT at 5% gain, and **(A″)** merged signals. Scale bar = 100 µm.

Extended Data Figure 2. Duplexed two-photon imaging of *Drosophila* brain stained with ATTO 490LS and Alexa Fluor 488 at different laser powers and detector gains.

Resource Type: Image

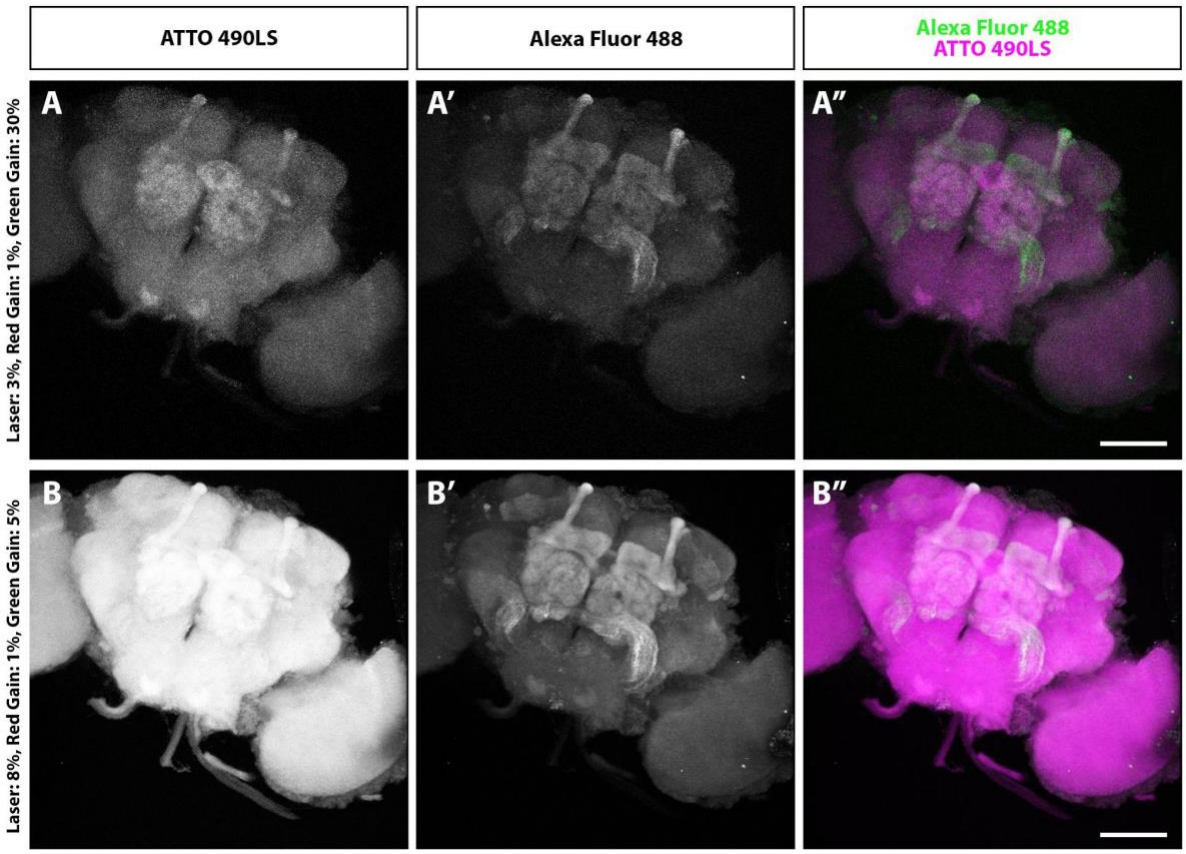

(A–A″) Maximum intensity projection images of an ATTO 490LS- and Alexa Fluor 488-coupled-anti-c-Myc tag antibody-stained *elav-Gal4>UAS-TID-Dlg1 Drosophila* brain. Both fluorophores were simultaneously excited by the 920 nm laser at 3% power (30 mW). Detection of **(A)** ATTO 490LS signals with the red-filtered PMT at 1% gain, **(A′)** detection of Alexa Fluor 488 signals with the green-filtered PMT at 30% gain, and **(A″)** merged signals. Scale bar = 100 µm. **(B–B″)** The same experiment as in **A–A″**, but fluorophores were instead simultaneously excited by the 920 nm laser at 8% power (80 mW). Detection of **(B)** ATTO 490LS signals with the red-filtered PMT at 1% gain, **(B′)** detection of Alexa Fluor 488 signals with the green-filtered PMT at 5% gain, and **(B″)** merged signals. Scale bar = 100 µm.

Extended Data Movie 1. *Z*-stack of two-photon image of *Drosophila* brain stained with ATTO 490LS and Alexa Fluor 488.

Resource Type: Movie
Z-stack of the supplementary two-photon image.

Extended Data Movie 2. 3D rendering of two-photon image of *Drosophila* brain stained with ATTO 490LS and Alexa Fluor 488.

Resource Type: Movie
3D rendering of the supplementary two-photon image.

Acknowledgements

We thank Gunnar Heiko Dirk Poplawski and Keshika Ravichandran (Programme in Neuroscience and Behavioural Disorders, Duke-NUS Medical School) for sharing the unpublished *UAS-TID-Dlg1* flies. We thank Sukanya Shyama Sundar (Multiphoton Core Facility — Multiphoton Microscopy Unit, Yong Loo Lin School of Medicine, National University of Singapore) for their technical support during the early stages of the project. We thank Stanislav Ott, Hyunsoo Shawn Je (Programme in Neuroscience and Behavioural Disorders, Duke-NUS Medical School), and Sangyu Xu (Institute of Molecular and Cell Biology, A*STAR) for insightful and productive discussions.

Funding

K.Y.C., X.Z., D.D.S., and A.C-C. were supported by the OFYIRG20nov-0024 grant from the National Medical Research Council, Singapore, by grants MOE-T2EP30222-0018 and MOE-T2EP30223-0009 from the Ministry of Education, Singapore, and by a Duke-NUS Medical School grant. X.Z. and A.C-C. were supported by FY2022-MOET1-0001.

Author Contributions

King Yee Cheung: conceptualisation, methodology, investigation, data curation, formal analysis, visualisation, writing — original draft, writing — reviewing and editing
Yue Wu: methodology, investigation, data curation, validation
Shu Ying Lee: conceptualisation, methodology

Xianyuan Zhang: investigation, writing — reviewing and editing
Masahiro Fukuda: investigation, writing — reviewing and editing
Danesha Devini Suresh: conceptualisation, writing — reviewing and editing
Adam Claridge-Chang: conceptualisation, supervision, funding acquisition, writing — reviewing and editing

300 **References**

301 Branon, T. C., Bosch, J. A., Sanchez, A. D., Udeshi, N. D., Svinkina, T., Carr, S. A., et al.
302 (2018). Efficient proximity labeling in living cells and organisms with TurboID. *Nat.*
303 *Biotechnol.* 36, 880–887. doi: 10.1038/nbt.4201

304 Hao, Y. A., Lee, S., Roth, R. H., Natale, S., Gomez, L., Taxidis, J., et al. (2024). A fast and
305 responsive voltage indicator with enhanced sensitivity for unitary synaptic events.
306 *Neuron* 112, 3680–3696.e8. doi: 10.1016/j.neuron.2024.08.019

307 Kim, B. B., Wu, H., Hao, Y. A., Pan, M., Chavarha, M., Zhao, Y., et al. (2022). A red
308 fluorescent protein with improved monomericity enables ratiometric voltage imaging
309 with ASAP3. *Sci. Rep.* 12, 3678. doi: 10.1038/s41598-022-07313-1

310 Lahey, T., Gorczyca, M., Jia, X. X., and Budnik, V. (1994). The Drosophila tumor suppressor
311 gene dlg is required for normal synaptic bouton structure. *Neuron* 13, 823–835. doi:
312 10.1016/0896-6273(94)90249-6

313 Lakowicz, J. R. (2001). Radiative decay engineering: biophysical and biomedical
314 applications. *Anal. Biochem.* 298, 1–24. doi: 10.1006/abio.2001.5377

315 Likhotkin, I., Lincoln, R., Bossi, M. L., Butkevich, A. N., and Hell, S. W. (2023).
316 Photoactivatable large Stokes shift fluorophores for multicolor nanoscopy. *J. Am.*
317 *Chem. Soc.* 145, 1530–1534. doi: 10.1021/jacs.2c12567

318 Liu, H., Jiang, G., Ke, G., Ren, T.-B., and Yuan, L. (2024). Organic fluorophores with large
319 Stokes shift for bioimaging and biosensing. *ChemPhotoChem* 8. doi:
320 10.1002/cptc.202300277

321 Liu, Z., Lu, X., Villette, V., Gou, Y., Colbert, K. L., Lai, S., et al. (2022). Sustained deep-tissue
322 voltage recording using a fast indicator evolved for two-photon microscopy. *Cell* 185,
323 3408–3425.e29. doi: 10.1016/j.cell.2022.07.013

324 Los, G. V., Encell, L. P., McDougall, M. G., Hartzell, D. D., Karassina, N., Zimprich, C., et al.
325 (2008). HaloTag: a novel protein labeling technology for cell imaging and protein
326 analysis. *ACS Chem. Biol.* 3, 373–382. doi: 10.1021/cb800025k

327 Marques, S. M., Slanska, M., Chmelova, K., Chaloupkova, R., Marek, M., Clark, S., et al.
328 (2022). Mechanism-based strategy for optimizing HaloTag protein labeling. *JACS Au* 2,
329 1324–1337. doi: 10.1021/jacsau.2c00002

330 Nakai, J., Ohkura, M., and Imoto, K. (2001). A high signal-to-noise Ca2+ probe composed of
331 a single green fluorescent protein. *Nat. Biotechnol.* 19, 137–141. doi: 10.1038/84397

332 Reitz, S. J., Sauerbeck, A. D., and Kummer, T. T. (2021). Enhanced multiplexing of
333 immunofluorescence microscopy using a long Stokes shift fluorophore. *Curr. Protoc.* 1,
334 e214. doi: 10.1002/cpz1.214

335 Schindelin, J., Arganda-Carreras, I., Frise, E., Kaynig, V., Longair, M., Pietzsch, T., et al.
336 (2012). Fiji: an open-source platform for biological-image analysis. *Nat. Methods* 9,
337 676–682. doi: 10.1038/nmeth.2019

Schmid, B., Schindelin, J., Cardona, A., Longair, M., and Heisenberg, M. (2010). A high-level 3D visualization API for Java and ImageJ. *BMC Bioinformatics* 11, 274–274. doi: 10.1186/1471-2105-11-274

Sednev, M. V., Belov, V. N., and Hell, S. W. (2015). Fluorescent dyes with large Stokes shifts for super-resolution optical microscopy of biological objects: a review. *Methods Appl. Fluoresc.* 3, 042004. doi: 10.1088/2050-6120/3/4/042004

Shiffman, D. (2015). *Learning processing*. Oxford, England: Morgan Kaufmann. doi: 10.1016/c2011-0-69691-7

Stokes, G. G. (1852). XXX. On the change of refrangibility of light. *Philos. Trans. R. Soc. Lond.* 142, 463–562. doi: 10.1098/rstl.1852.0022

Subach, O. M., Vlaskina, A. V., Agapova, Y. K., Piatkevich, K. D., Patrushev, M. V., Samygina, V. R., et al. (2022). LSSmScarlet2 and LSSmScarlet3, Chemically Stable Genetically Encoded Red Fluorescent Proteins with a Large Stokes' Shift. *Int. J. Mol. Sci.* 23. doi: 10.3390/ijms231911051

Thorlabs (United States). (2010). "Thorlabs MPM200 Multiphoton Microscope Operating Manual". Thorlabs. doi:10.5281/zenodo.17895580.

Valeur, B. (2001). *Molecular fluorescence: Principles and applications*. Weinheim: Wiley-VCH Verlag GmbH. doi: 10.1002/3527600248

Woods, D. F., Hough, C., Peel, D., Callaini, G., and Bryant, P. J. (1996). Dlg protein is required for junction structure, cell polarity, and proliferation control in Drosophila epithelia. *J. Cell Biol.* 134, 1469–1482. doi: 10.1083/jcb.134.6.1469

Zhang, Y., Rózsa, M., Liang, Y., Bushey, D., Wei, Z., Zheng, J., et al. (2023). Fast and sensitive GCaMP calcium indicators for imaging neural populations. *Nature* 615, 884–891. doi: 10.1038/s41586-023-05828-9

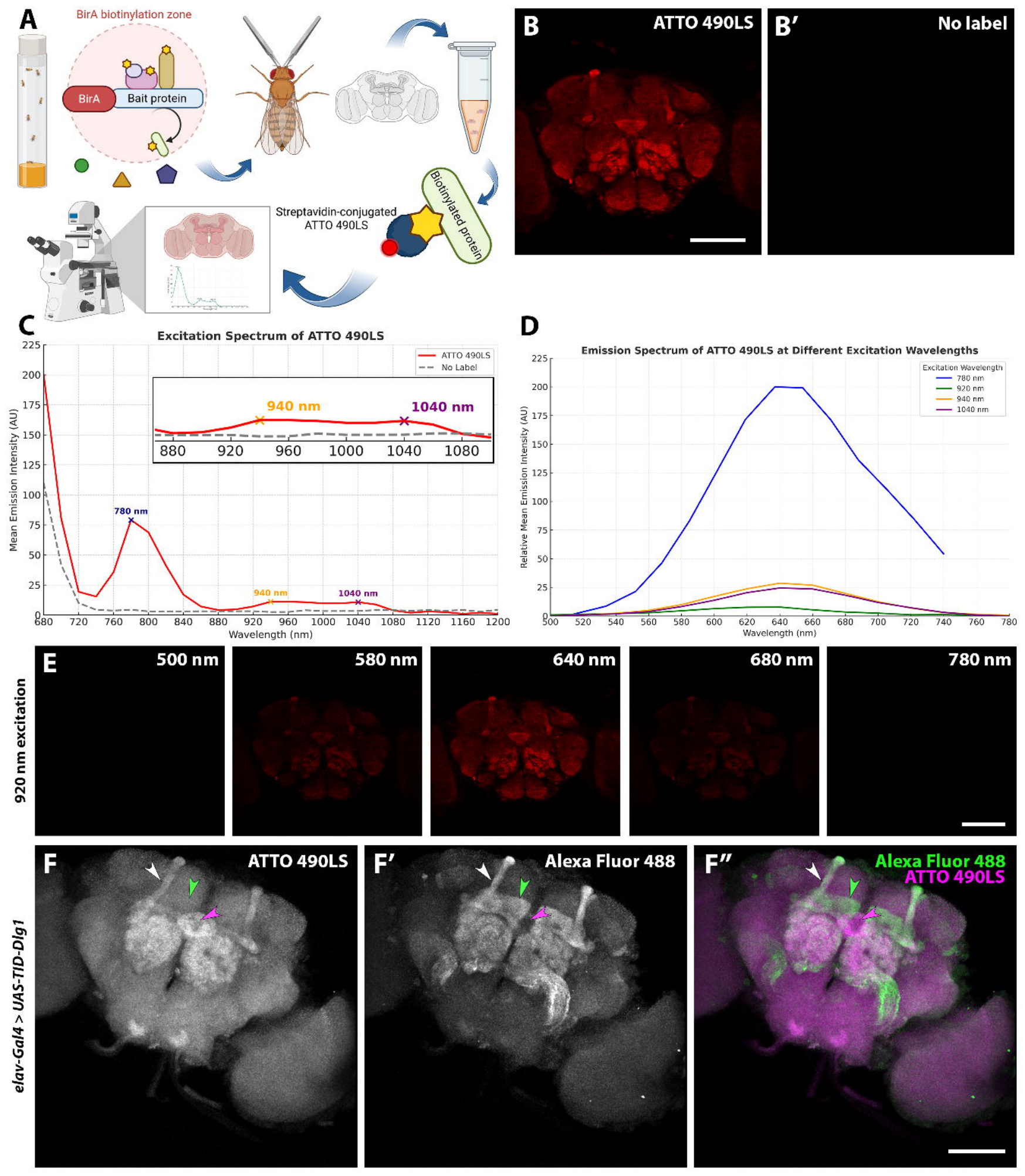
A
BirA biotinylation zone
BirA
Bait protein
Streptavidin-conjugated
ATTO 490LS
Biotinylated protein
B
ATTO 490LS
B′
No label
C
Excitation Spectrum of ATTO 490LS
ATTO 490LS
No Label
940 nm
1040 nm
780 nm
Mean Emission Intensity (AU)
Wavelength (nm)
D
Emission Spectrum of ATTO 490LS at Different Excitation Wavelengths
Excitation Wavelength
780 nm
920 nm
940 nm
1040 nm
Relative Mean Emission Intensity (AU)
Wavelength (nm)
E
500 nm
580 nm
640 nm
680 nm
780 nm
920 nm excitation
F
ATTO 490LS
F′
Alexa Fluor 488
F″
Alexa Fluor 488
ATTO 490LS
elav-Gal4 > UAS-TID-Dlg1